

Article

Screening of Omicron Virus Strain by Quantifying the Spike Protein Content

Zhenyu He ^{1,†}, Hengzhen Chang ^{1,†}, Yichuan Wang ¹, Siman Xie ¹, Yingwei Liu ¹, Yuxiu Zhao ¹, Na Li ^{1,*} and Yuntao Zhang ^{2,*}

¹ Beijing Institute of Biological Products Company Limited, Beijing 100176, China; hezhenyu@sinopharm.com (Z.H.); changhengzhen@sinopharm.com (H.C.); wangyichuan@sinopharm.com (Y.W.); xiesiman@sinopharm.com (S.X.); liuyingwei@sinopharm.com (Y.L.); zhaoyuxiu1@sinopharm.com (Y.Z.)

² China National Biotec Group Company Limited, Beijing 100024, China

* Correspondence: lina1@sinopharm.com (N.L.); zhangyuntao@sinopharm.com (Y.Z.)

[†] These authors contributed equally to this work.

Abstract: In the development of an inactivated virus vaccine, the isolation of a single virus strain plays a key role in determining potency. The conventional methods of quantification of virus number are mainly based on virus titers, which are subjective and time-consuming, especially in the early stage of virus isolation, in which the titer difference is weak. Previous reports have shown a high correlation between the spike protein and the potency of COVID-19 vaccines. In this paper, we report a novel, fast, and convenient method of screening an Omicron virus strain by quantifying the spike protein content, where the isolated strain shows high affinity to Omicron-specific antibodies and a high titer, and it can induce high levels of neutralization antibodies.

Keywords: screening of Omicron virus strain; virus titer; quantify the spike protein content



Citation: He, Z.; Chang, H.; Wang, Y.; Xie, S.; Liu, Y.; Zhao, Y.; Li, N.; Zhang, Y. Screening of Omicron Virus Strain by Quantifying the Spike Protein Content. *COVID* **2024**, *4*, 838–847. <https://doi.org/10.3390/covid4060056>

Academic Editor: Roger Frutos

Received: 14 May 2024

Revised: 8 June 2024

Accepted: 16 June 2024

Published: 20 June 2024



Copyright: © 2024 by the authors. Licensee MDPI, Basel, Switzerland. This article is an open access article distributed under the terms and conditions of the Creative Commons Attribution (CC BY) license (<https://creativecommons.org/licenses/by/4.0/>).

1. Introduction

The Omicron BA.1 variant was first identified in South Africa in November 2021 [1] and was distinct for its 35 mutations in the spike protein [2,3], but with the increasing mutation sites of the novel variants recently identified, the immune escape capacity of the mutant strains has also increased. New variants and mutations have appeared continuously in the Omicron family, such as the evolved BA.5 strain [4,5], the XBB.1.5 strain [6,7], and JN.1 [8,9].

Vaccines are an effective way to prevent COVID-19 [10], and the current COVID-19 vaccine candidates are mainly based on the following technical routes: inactivated virus vaccines [11,12], protein subunit vaccines [13,14], mRNA vaccines [15,16], and viral vector vaccines [17], such as the adenoviral vector vaccine [18,19]. Among the 7.3 billion COVID-19 vaccine doses that have been delivered globally, inactivated virus vaccines represent almost half. These vaccines played an important role in significantly reducing rates of hospitalization, severe illness, and mortality [11,12,20,21].

The isolation of a virus strain is vital during the development of inactivated virus vaccines [22]. In addition, the selection of a superior strain with high virulence and high potency is crucial to the quality of the vaccine. A single virus strain is usually achieved by limited dilutions [23,24] or plaque cloning [25,26] in a sensitive cell line. To further quantify the number of isolated viruses, a variety of assays have been developed [27], such as direct visualization by transmission electron microscopy (TEM) [28], the quantification of genomic material by quantitative real-time polymerase chain reaction (qPCR) [28], plaque assays [29,30], and endpoint dilution assays [31]. The former two assays cannot reflect the virus infectivity (usually referred to as the virus titer), while the latter two mainly rely on the appearance of visible cell cytopathic effects (CPEs), which is time-consuming.

TEM is expensive and has low accuracy, while qPCR is based on the genomic material, and the viral genome is usually produced in excess [28]. The endpoint dilution assay usually requires one week to complete, while the plaque assay takes up to two weeks [28]. In addition, the results of these two assays are subjective. In the early stage of virus isolation, the difference in titer of the selected strain was not significant, which was not conducive to rapid identification, and more passages were needed to distinguish them. The most important factor in inactivated virus vaccines is the protein content of key antigens. Therefore, there is an urgent need for a fast and precise assay that reflects the quantity of key antigens and affects the speed of virus isolation, further affecting the overall speed of vaccine development.

In this paper, we report a novel method to quantify the spike protein content that can be applied to rapid screening of the Omicron variant. Compared with conventional methods based on titer (each round requires at least one week), this novel method only requires less than 24 h, and it is easy to perform and economical. Specifically, we quantify the content of the spike protein using Western blot and choose the strain with the highest concentration. The spike protein is key to viral entry into cells [32] and contains multiple epitopes that induce antibody neutralization [33]. The Omicron strain isolated by the quantification of the spike protein shows high affinity to Omicron-specific antibodies and shows high titer, and it can induce high antibody neutralization, which is ideal and provides a new method for virus isolation in further studies.

2. Methods

2.1. Animals

BALB/c mice weighing 18–20 g were purchased from Beijing Weitonglihua Experimental Animal Technology Co., Ltd. (Beijing, China). They were healthy and provided with an SPF environment (12 h light/dark cycle; temperature 20–26 °C; humidity 40–70%).

2.2. Animal Ethics Statement

All animals involved in this study were housed and cared for in a facility accredited by the Association for the Assessment and Accreditation of Laboratory Animal Care (AAALAC). All experimental procedures with mice were conducted according to United States Department of Agriculture (USDA) Animal Welfare Regulations (Public Law 99–198) [34] and were approved by the Institutional Animal Care and Use Committee (IACUC). The approval code and date are BSYF20220903005 and 3 September 2022, respectively.

2.3. Virus Strains and Potential Vaccine Development

The Omicron strain HK-OM-P0 was isolated from a patient's pharyngeal swab and then isolated and cultured to obtain single-clone virus strains (P1, #1, #3, #4, #5, and #11) using plaque purification, which was based on agarose (3%) and M199 culture medium (Gibco, New York, NY, USA).

All P1 strains were further cultured in a 10 L basket bioreactor at a temperature of 36 ± 1 °C. The virus solution was harvested 48–72 h after inoculation and was then inactivated with b-propiolactone at a ratio of 1:4000 at 2–8 °C for 20–24 h, followed by chromatography purification. The final bulk was prepared by adding aluminum hydroxide as the adjuvant in PBS buffer for mice immunization.

2.4. Lowry Method

The protein content was determined using the Lowry method in accordance with the relevant requirements of the general chapters of "Chinese Pharmacopoeia" Part 3 (2020 Edition) [35]. Briefly, a standard protein solution and virus samples were diluted to appropriate concentrations, and then an alkaline copper solution was added and mixed evenly at room temperature for 10 min, followed by the addition of phenol reagent at room temperature for 20–30 min. The absorbance was measured at a wavelength of 650 nm, and

the data were fitted to the linear regression equation based on the concentration of the reference solution and its corresponding absorbance.

2.5. Western Blot

Samples containing 10 µg of total protein were mixed with a loading buffer and then boiled at 100 °C for 10 min. Proteins were separated using 12% sodium dodecyl sulfate-polyacrylamide gel electrophoresis (SDS-PAGE) and transferred to a PVDF membrane. The membrane was sealed in 5% skim milk in PBST for 2 h at 37 °C, followed by overnight incubation with an anti-S protein rabbit polyclonal antibody (Sino-Biological, 1:1000, Beijing, China) at 4 °C. The membrane was incubated with the secondary antibody goat anti-rabbit IgG (HRP) (GE, 1:4000, Boston, MA, USA) for 1 h at room temperature and exposed to the Image Quant TL system for imaging analysis.

2.6. Antigen Analysis Based on Multiclonal Antibody ELISA

The antigenic content was measured based on the ELISA method using a multiclonal antibody. The “homemade” polyclonal antibody was created using the following steps: First, guinea pigs and rabbits were immunized against the SARS-CoV-2 B.1.1.529 (Omicron) S1 and S2 trimer protein (Sino Biological, 40589-V08H26), respectively, and the serum was collected for titer detection. The serum with a high titer was purified to obtain the polyclonal antibody, and the guinea pig polyclonal antibody was the capture antibody, while the rabbit polyclonal antibody was the detection antibody.

The homemade guinea pig anti-S protein polyclonal antibodies were precoated on a plate. The virus species samples diluted with a PBS solution containing 1% BSA and 0.05% Tween-20 were added, followed by incubation at 37 °C for 1 h. After washing five times, the homemade rabbit anti-S protein polyclonal antibodies were added for incubation for 60 min at room temperature. Then, the plate was washed five times, followed by the addition of a donkey anti-rabbit IgG-Peroxidase antibody (Cytiva, NA934V, Washington, DC, USA) for incubation for 1 h at 37 °C. After washing 5 times, TMB (BIBP, Beijing, China) chromogenic solution was added to react for 10 min at 37 °C before being stopped by termination solution. The absorbance was measured at 450 and 630 nm using a microplate reader. IC₅₀ was calculated using GraphPad Prism 8.3.0 for three-parameter logistic curve fitting.

2.7. Antigen Analysis Based on Monoclonal Antibody ELISA

The antigenic content was also measured using Omicron-specific antibodies. The main methods are identical to the steps of the multiclonal antibody ELISA, with the exception of the homemade rabbit anti-S protein polyclonal antibodies, which were replaced by Omicron-specific antibodies (Acro SPD-M415, 1:20,000, Beijing, China), and donkey anti-rabbit IgG-Peroxidase antibodies, which were replaced by goat anti-mouse IgG peroxidase antibodies from another manufacturer (Jackson 148979, 1:2000, Lancaster, PA, USA).

2.8. Virus Titer Detection

The virus titer was detected using the microplate cytopathic effect. Specifically, the virus was ten-fold serially diluted with 199 medium (Gibco, New York, NY, USA) containing 10% bovine serum (Minhai Bio, Lanzhou, China) and inoculated in 96-well plates; then, a Vero cell suspension was seeded at 2×10^5 cells/mL and incubated in a 37 °C and 5% CO₂ environment for 4 days. The virus titer was calculated using the Karber method [36].

2.9. Surface Plasmon Resonance

Surface plasmon resonance (SPR) experiments were performed on the Biacore 8K (Cytiva). To detect the dissociation coefficients between the anti-SARS-CoV-2 spike RBD antibody (Omicron-specific) (Acro Biosystem; AS113, Beijing, China) and purified virus, up to ~200 RU of the antibody was captured on a Series S Sensor Protein A Chip (Cytiva). Virus strains 4 and 3 were serially diluted, ranging from 6.25 to 400 nM (2-fold dilutions), and then injected. The running buffer was 0.01 M HEPES, pH 7.4, 150 mM NaCl, 3 mM

EDTA, and supplemented with 0.005% Tween-20. The data were fitted to a 1:1 binding model using Biacore Evaluation Software (version number: 3.0.12.15655).

2.10. Immunogenicity Analysis

The vaccine was prepared by mixing the aluminum hydroxide adjuvant with purified virus and injected into BALB/c mice. The vaccine was administered on D0 (6 µg/dose, 0.5 mL), and the blood was collected on D14. The neutralization assay was based on the microplate CPE (micro-cytopathogenic efficiency) method as described before [11]. The virus strain for the neutralization assay was Omicron BA.1, which was isolated from the patient’s pharyngeal swab.

2.11. Statistical Analysis

All statistical analyses were performed using GraphPad Prism 8. In a comparison between the two groups, a two-tailed Mann–Whitney test was used to determine significance. Error bars represent SEM. * $p < 0.05$; ** $p < 0.01$; *** $p < 0.001$.

3. Results

3.1. Spike Protein Content Analysis

The spike protein is the main antigen of SARS-CoV-2, and its receptor binding domain has a strong binding ability to the angiotensin-converting enzyme receptor (ACE2). Table 1 shows the result of the whole protein content, and Figure 1 shows the content of spike protein by loading the same amount of whole protein (total 10 µg).

Table 1. Summary of protein content of screened virus species.

Virus Strain	Protein Content (µg/mL)
#1	2639.79
#3	2513.62
#4	2429.51
#5	2322.45
#11	2555.68

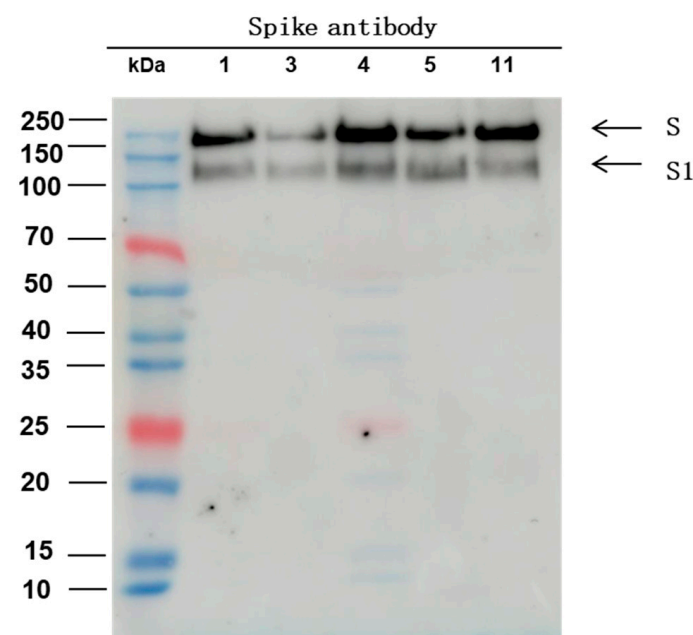


Figure 1. Western blot result: The spike protein content of five Omicron virus strains were evaluated by incubating with antibodies targeting S protein.

The results in Figure 1 and Table 1 show that virus strains 4 and 11 show potential as vaccine candidates due to the high content of spike protein, while virus strain 3 is the worst.

To further confirm the antigen content of the spike protein, we first used the Lowry method to determine the protein content. The antigen content present in the total protein is correlated with the half maximal inhibitory concentration (IC_{50}). A higher antigen content reflects a lower IC_{50} number. The multiclonal antibody results are displayed in Figure 2a. Consistent with the results from Western blots, the IC_{50} of virus strains 4 and 11 is 167.9 $\mu\text{g}/\text{mL}$ and 241.9 $\mu\text{g}/\text{mL}$, respectively, which is smaller than that of virus strain 3 (511.1 $\mu\text{g}/\text{mL}$). This reflects the fact that the antigen content of virus strains 4 and 11 is higher than that of virus strain 3. We also selected an Omicron-specific monoclonal antibody to incubate with virus strains 4, 11, and 3 (see Figure 2b), and the results showed that the IC_{50} of virus strain 3 is 72.98 $\mu\text{g}/\text{mL}$, which is 5-fold that of virus strain 4 (14.53 $\mu\text{g}/\text{mL}$).

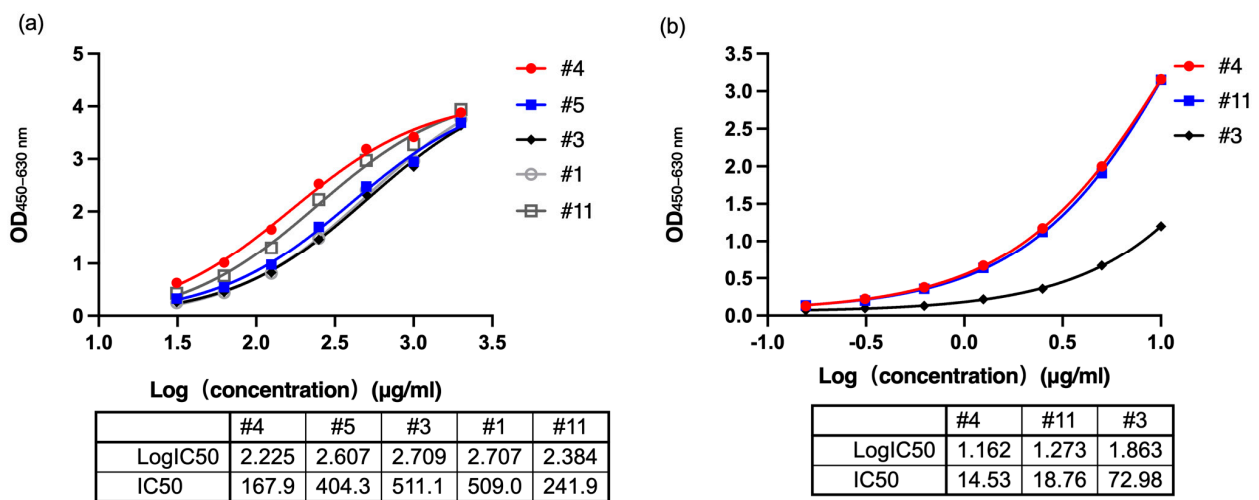


Figure 2. The antigen content determined by ELISA. (a) The IC_{50} between virus strains 1, 3, 4, 5, and 11 and homemade multiclonal antibody; (b) the IC_{50} between virus strains 3, 4, and 11 and Omicron-specific monoclonal antibody.

3.2. Affinity Analysis

Consistent with the Western blot results and antigen content, virus strain 4 showed higher affinities with the anti-SARS-CoV-2 spike RBD antibody (Omicron-specific) in comparison with virus strain 3 (Figure 3). Specifically, the equilibrium dissociation constant (K_D) of the Omicron-specific anti-RBD antibody and virus strain 4 is 14 nM, and that of this antibody and virus strain 3 is 572 nM, which is a 40-fold increase in affinity, reinforcing the fact that virus strain 4 is more suitable as a candidate for vaccine development.

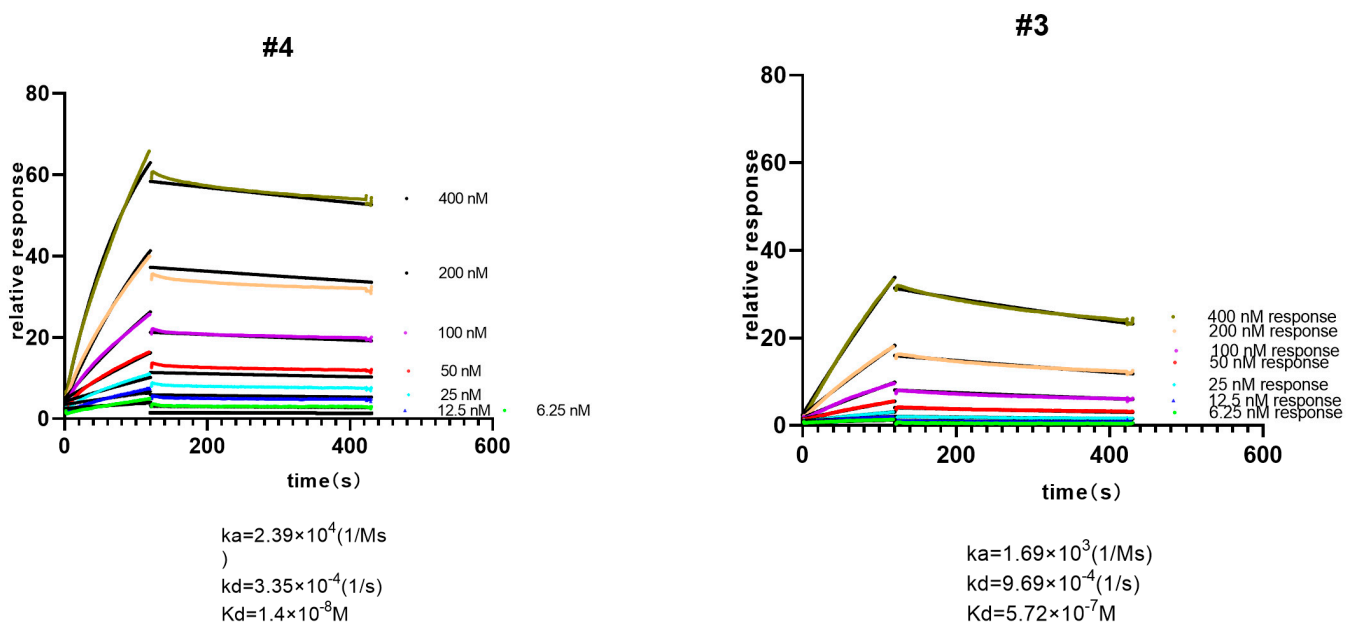


Figure 3. Binding curves of anti-SARS-CoV-2 spike RBD antibody (Omicron-specific) with virus strains 4 (left) and 3 (right). Data are shown as lines of different colors, and the best fit of the data to a 1:1 binding model is shown in black.

3.3. Virus Titer Analysis

The micro-cytopathic effect method (CPE) was used for titer screening to analyze the infectivity of Omicron strains, and the results (Table 2) showed that the titer of virus strain 4 was higher than that of virus strain 3, which was consistent with the result from the quantification assay. However, those of virus strains 1, 3, 5, and 11 were identical, reflecting the insensitivity of the CPE method and indicating the difference in the total amount of virus as the CPE only measures the amount of infective virus.

Table 2. Summary of titration results from five Omicron strains.

Type	10^{-2}	10^{-3}	10^{-4}	10^{-5}	Titer (LgCCID ₅₀ /mL)
#1	8/8	5/8	0/8	0/8	4.125
#3	8/8	5/8	0/8	0/8	4.125
#4	8/8	8/8	1/8	0/8	4.625
#5	8/8	5/8	0/8	0/8	4.125
#11	8/8	5/8	0/8	0/8	4.125

3.4. Neutralizing Antibody Analysis

The results (Figure 4) showed that the neutralization geometric mean titer (GMT) (virus strain 4) against Omicron was about 219, while the neutralization geometric mean titer (GMT) (virus strain 3) against Omicron was about 100. This indicates that this virus strain 4 could induce a significantly higher neutralizing antibody titer than virus strain 3 (p value = 0.0038), which is consistent with the previous results.

paper can be used to rapidly screen inactivated virus vaccine strains based on the content of effective antigens on the surface of the strains.

Author Contributions: Study design: N.L. and Y.Z. (Yuntao Zhang); Investigation: N.L., Y.Z. (Yuntao Zhang), Z.H., and H.C.; Methodology: all authors; Writing the manuscript: Z.H., H.C., Y.W., S.X. and Y.L.; Supervision, N.L., Y.Z. (Yuxiu Zhao) and Y.Z. (Yuntao Zhang); Project Administration, N.L. and Y.Z. (Yuntao Zhang). All authors have read and agreed to the published version of the manuscript.

Funding: This work was supported by funding from the National Key Research and Development Program of China (2023YFE0203400).

Institutional Review Board Statement: The animal study was approved by the Institutional Animal Care and Use Committee (IACUC). The approval code and date are BSYF20220903005 and 3 September 2022, respectively.

Informed Consent Statement: Not applicable.

Data Availability Statement: Data are contained within the article.

Conflicts of Interest: The authors declare no conflict of interest.

References

- Viana, R.; Moyo, S.; Amoako, D.G.; Tegally, H.; Scheepers, C.; Althaus, C.L.; Anyaneji, U.J.; Bester, P.A.; Boni, M.F.; Chand, M.; et al. Rapid epidemic expansion of the SARS-CoV-2 Omicron variant in southern Africa. *Nature* **2022**, *603*, 679–686. [[CrossRef](#)] [[PubMed](#)]
- Garcia-Beltran, W.F.; St Denis, K.J.; Hoelzemer, A.; Lam, E.C.; Nitido, A.D.; Sheehan, M.L.; Berrios, C.; Ofoman, O.; Chang, C.C.; Hauser, B.M.; et al. mRNA-based COVID-19 vaccine boosters induce neutralizing immunity against SARS-CoV-2 Omicron variant. *medRxiv* **2021**, 14:2021.12.14.21267755, Update in: *Cell* **2022**, *185*, 457–466.e4. [[CrossRef](#)] [[PubMed](#)] [[PubMed Central](#)]
- Berkhout, B.; Herrera-Carrillo, E. SARS-CoV-2 Evolution: On the Sudden Appearance of the Omicron Variant. *J. Virol.* **2022**, *96*, e0009022. [[CrossRef](#)] [[PubMed](#)]
- Tegally, H.; Moir, M.; Everatt, J.; Giovanetti, M.; Scheepers, C.; Wilkinson, E.; Subramoney, K.; Makatini, Z.; Moyo, S.; Amoako, D.G.; et al. Emergence of SARS-CoV-2 Omicron lineages BA.4 and BA.5 in South Africa. *Nat. Med.* **2022**, *28*, 1785–1790. [[CrossRef](#)]
- Tuekprakhon, A.; Nutalai, R.; Djokaite-Guraliuc, A.; Zhou, D.; Ginn, H.M.; Selvaraj, M.; Liu, C.; Mentzer, A.J.; Supasa, P.; Duyvesteyn, H.M.; et al. Antibody escape of SARS-CoV-2 Omicron BA.4 and BA.5 from vaccine and BA.1 serum. *Cell* **2022**, *185*, 2422–2433.e13. [[CrossRef](#)] [[PubMed](#)]
- Yue, C.; Song, W.; Wang, L.; Jian, F.; Chen, X.; Gao, F.; Shen, Z.; Wang, Y.; Wang, X.; Cao, Y. ACE2 binding and antibody evasion in enhanced transmissibility of XBB.1.5. *Lancet Infect. Dis.* **2023**, *23*, 278–280. [[CrossRef](#)] [[PubMed](#)]
- Parums, D.V. Editorial: The XBB.1.5 ('Kraken') Subvariant of Omicron SARS-CoV-2 and its Rapid Global Spread. *Med. Sci. Monit.* **2023**, *29*, e939580. [[CrossRef](#)] [[PubMed](#)]
- Kaku, Y.; Okumura, K.; Padilla-Blanco, M.; Kosugi, Y.; Uriu, K.; Hinay, A.A.; Chen, L.; Plianchaisuk, A.; Kobiyama, K.; Ishii, K.J.; et al. Virological characteristics of the SARS-CoV-2 JN.1 variant. *Lancet Infect. Dis.* **2024**, *24*, e82. [[CrossRef](#)]
- Yang, S.; Yu, Y.; Xu, Y.; Jian, F.; Song, W.; Yisimayi, A.; Wang, P.; Wang, J.; Liu, J.; Yu, L.; et al. Fast evolution of SARS-CoV-2 BA.2.86 to JN.1 under heavy immune pressure. *Lancet Infect. Dis.* **2024**, *24*, e70–e72. [[CrossRef](#)] [[PubMed](#)]
- Zhang, Y.; Zhao, Y.; Liang, H.; Xu, Y.; Zhou, C.; Yao, Y.; Wang, H.; Yang, X. Innovation-driven trend shaping COVID-19 vaccine development in China. *Front. Med.* **2023**, *17*, 1096–1116. [[CrossRef](#)] [[PubMed](#)]
- Wang, H.; Zhang, Y.; Huang, B.; Deng, W.; Quan, Y.; Wang, W.; Xu, W.; Zhao, Y.; Li, N.; Zhang, J.; et al. Development of an Inactivated Vaccine Candidate, BBIBP-CorV, with Potent Protection against SARS-CoV-2. *Cell* **2020**, *182*, 713–721.e9. [[CrossRef](#)] [[PubMed](#)]
- Jin, L.; Li, Z.; Zhang, X.; Li, J.; Zhu, F. CoronaVac: A review of efficacy, safety, and immunogenicity of the inactivated vaccine against SARS-CoV-2. *Hum. Vaccines Immunother.* **2022**, *18*, 2096970. [[CrossRef](#)] [[PubMed](#)]
- Bravo, L.; Smolenov, I.; Han, H.H.; Li, P.; Hosain, R.; Rockhold, F.; Clemens, S.A.C.; Roa, C.; Borja-Tabora, C.; Quinsa, A.; et al. Efficacy of the adjuvanted subunit protein COVID-19 vaccine, SCB-2019: A phase 2 and 3 multicentre, double-blind, randomised, placebo-controlled trial. *Lancet* **2022**, *399*, 461–472. [[CrossRef](#)] [[PubMed](#)]
- Dai, L.; Gao, L.; Tao, L.; Hadinegoro, S.R.; Erkin, M.; Ying, Z.; He, P.; Girsang, R.T.; Vergara, H.; Akram, J.; et al. Efficacy and Safety of the RBD-Dimer-Based COVID-19 Vaccine ZF2001 in Adults. *N. Engl. J. Med.* **2022**, *386*, 2097–2111. [[CrossRef](#)] [[PubMed](#)]
- Schlake, T.; Thess, A.; Fotin-Mleczek, M.; Kallen, K.J. Developing mRNA-vaccine technologies. *RNA Biol.* **2012**, *9*, 1319–1330. [[CrossRef](#)] [[PubMed](#)]
- Polack, F.P.; Thomas, S.J.; Kitchin, N.; Absalon, J.; Gurtman, A.; Lockhart, S.; Perez, J.L.; Pérez Marc, G.; Moreira, E.D.; Zerbini, C.; et al. Safety and Efficacy of the BNT162b2 mRNA COVID-19 Vaccine. *N. Engl. J. Med.* **2020**, *383*, 2603–2615. [[CrossRef](#)] [[PubMed](#)]

17. Soleimanpour, S.; Yaghoubi, A. COVID-19 vaccine: Where are we now and where should we go? *Expert. Rev. Vaccines* **2021**, *20*, 23–44. [[CrossRef](#)] [[PubMed](#)]
18. Ramasamy, M.N.; Minassian, A.M.; Ewer, K.J.; Flaxman, A.L.; Folegatti, P.M.; Owens, D.R.; Voysey, M.; Aley, P.K.; Angus, B.; Babbage, G.; et al. Safety and immunogenicity of ChAdOx1 nCoV-19 vaccine administered in a prime-boost regimen in young and old adults (COV002): A single-blind, randomised, controlled, phase 2/3 trial. *Lancet* **2021**, *396*, 1979–1993. [[CrossRef](#)] [[PubMed](#)]
19. Sadoff, J.; Gray, G.; Vandebosch, A.; Cárdenas, V.; Shukarev, G.; Grinsztejn, B.; Goepfert, P.A.; Truyers, C.; Fennema, H.; Spiessens, B.; et al. Safety and Efficacy of Single-Dose Ad26.COV2.S Vaccine against COVID-19. *N. Engl. J. Med.* **2021**, *384*, 2187–2201. [[CrossRef](#)] [[PubMed](#)]
20. Al Kaabi, N.; Zhang, Y.; Xia, S.; Yang, Y.; Al Qahtani, M.M.; Abdulrazzaq, N.; Al Nusair, M.; Hassany, M.; Jawad, J.S.; Abdalla, J.; et al. Effect of 2 Inactivated SARS-CoV-2 Vaccines on Symptomatic COVID-19 Infection in Adults: A Randomized Clinical Trial. *JAMA* **2021**, *326*, 35–45. [[CrossRef](#)] [[PubMed](#)]
21. Bueno, S.M.; Abarca, K.; González, P.A.; Gálvez, N.M.S.; Soto, J.A.; Duarte, L.F.; Schultz, B.M.; Pacheco, G.A.; González, L.A.; Vázquez, Y.; et al. Safety and Immunogenicity of an Inactivated Severe Acute Respiratory Syndrome Coronavirus 2 Vaccine in a Subgroup of Healthy Adults in Chile. *Clin. Infect. Dis.* **2022**, *75*, e792–e804. [[CrossRef](#)] [[PubMed](#)]
22. Stelzer-Braid, S.; Walker, G.J.; Aggarwal, A.; Isaacs, S.R.; Yeang, M.; Naing, Z.; Stella, A.O.; Turville, S.G.; Rawlinson, W.D. Virus isolation of severe acute respiratory syndrome coronavirus 2 (SARS-CoV-2) for diagnostic and research purposes. *Pathology* **2020**, *52*, 760–763. [[CrossRef](#)] [[PubMed](#)]
23. Knowles, B.; Bonachela, J.A.; Cieslik, N.; Della Penna, A.; Diaz, B.; Baetge, N.; Behrenfeld, M.J.; Naumovitz, K.; Boss, E.; Graff, J.R.; et al. Altered growth and death in dilution-based viral predation assays. *PLoS ONE* **2023**, *18*, e0288114. [[CrossRef](#)] [[PubMed](#)]
24. Sugiyama, N.; Murayama, A.; Suzuki, R.; Watanabe, N.; Shiina, M.; Liang, T.J.; Wakita, T.; Kato, T. Single strain isolation method for cell culture-adapted hepatitis C virus by end-point dilution and infection. *PLoS ONE* **2014**, *9*, e98168. [[CrossRef](#)] [[PubMed](#)]
25. Gerganov, G.; Sürtmadzhiev, K. [Plaque cloning of the velogenic viscerotropic Newcastle disease virus]. *Vet. Med. Nauki* **1981**, *18*, 12–19. [[PubMed](#)]
26. Hirano, N.; Tawara, T.; Nomura, R.; Imai, A.; Ono, K.; Yamaguchi, R. Sensitive plaque assay and propagation of Chuzan (Kasba) virus, a Palyam serogroup orbivirus, in BHK-21 cells. *Zentralbl. Vet. B* **1996**, *43*, 333–342. [[CrossRef](#)] [[PubMed](#)]
27. Flint, J.S.; Enquist, L.W.; Shalka, A.M. Virological methods. In *Principles of Virology*, 3rd ed.; ASM: Almere, The Netherlands, 2009; Chapter 2.
28. Smither, S.J.; Lear-Rooney, C.; Biggins, J.; Pettitt, J.; Lever, M.S.; Olinger, G. Comparison of the plaque assay and 50% tissue culture infectious dose assay as methods for measuring filovirus infectivity. *J. Virol. Methods* **2013**, *193*, 565–571. [[CrossRef](#)]
29. Cooper, P.D. A method for producing plaques in agar suspensions of animal cells. *Virology* **1955**, *1*, 397–401. [[CrossRef](#)] [[PubMed](#)]
30. Dulbecco, R. Production of Plaques in Monolayer Tissue Cultures by Single Particles of an Animal Virus. *Proc. Natl. Acad. Sci. USA* **1952**, *38*, 747–752. [[CrossRef](#)] [[PubMed](#)]
31. Reed, L.J.; Muench, H. A simple method of estimating fifty per cent endpoints. *Am. J. Hyg.* **1938**, *27*, 493–497.
32. Lan, J.; Ge, J.; Yu, J.; Shan, S.; Zhou, H.; Fan, S.; Zhang, Q.; Shi, X.; Wang, Q.; Zhang, L.; et al. Structure of the SARS-CoV-2 spike receptor-binding domain bound to the ACE2 receptor. *Nature* **2020**, *581*, 215–220. [[CrossRef](#)] [[PubMed](#)]
33. Finkelstein, M.T.; Mermelstein, A.G.; Parker Miller, E.; Seth, P.C.; Stancovski, E.S.D.; Fera, D. Structural Analysis of Neutralizing Epitopes of the SARS-CoV-2 Spike to Guide Therapy and Vaccine Design Strategies. *Viruses* **2021**, *13*, 134. [[CrossRef](#)] [[PubMed](#)]
34. Public Law 99-198, Food Security Act of 1985, Subtitle F—Animal Welfare, U.S. DEP’T AGRIC. NAT’L AGRIC. LIBR. [Hereinafter Food Security Act of 1985]; See also Food Security Act of 1985 sec. 1752(a), § 13(2)(A). Available online: <https://www.nal.usda.gov/awic/public-law-99-198-foodsecurity-act-1985-subtitle-f-animal-welfare> (accessed on 20 October 2016).
35. National Pharmacopoeia Commission. *Pharmacopoeia of the People’s Republic of China: Part Three*; China Medical Technology Press: Beijing, China, 2020.
36. Zapata-Cardona, M.I.; Flórez-Álvarez, L.; Gómez-Gallego, D.M.; Moncada-Díaz, M.J.; Hernandez, J.C.; Díaz, F.; Rugeles, M.T.; Aguilar-Jiménez, W.; Zapata, W. Comparison among plaque assay, tissue culture infectious dose (TCID₅₀) and real-time RT-PCR for SARS-CoV-2 variants quantification. *Iran. J. Microbiol.* **2022**, *14*, 291–299. [[PubMed](#)]
37. Witt, A.S.A.; Trindade, G.d.S.; Gil de Souza, F.; Serafim, M.S.M.; da Costa, A.V.B.; Silva, M.V.F.; Iani, F.C.d.M.; Rodrigues, R.A.L.; Kroon, E.G.; Abrahão, J.S. Ultrastructural analysis of monkeypox virus replication in Vero cells. *J. Med. Virol.* **2023**, *95*, e28536. [[CrossRef](#)] [[PubMed](#)]
38. Mardanly, S.G.; Kazakov, A.A.; Demkin, V.V.; Zatevalov, A.M.; Mironov, A.Y. Development of a PCR assay for the detection of human herpes virus type 7. *Klin. Lab. Diagn.* **2022**, *67*, 658–662. [[CrossRef](#)] [[PubMed](#)]
39. Zhang, Y.; Tan, W.; Lou, Z.; Zhao, Y.; Zhang, J.; Liang, H.; Li, N.; Zhu, X.; Ding, L.; Huang, B.; et al. Vaccination with Omicron Inactivated Vaccine in Pre-vaccinated Mice Protects against SARS-CoV-2 Prototype and Omicron Variants. *Vaccines* **2022**, *10*, 1149. [[CrossRef](#)] [[PubMed](#)]
40. Cunningham, A.L.; Garçon, N.; Leo, O.; Friedland, L.R.; Strugnelli, R.; Laupèze, B.; Doherty, M.; Stern, P. Vaccine development: From concept to early clinical testing. *Vaccine* **2016**, *34*, 6655–6664. [[CrossRef](#)] [[PubMed](#)]
41. Delany, I.; Rappuoli, R.; De Gregorio, E. Vaccines for the 21st century. *EMBO Mol. Med.* **2014**, *6*, 708–720. [[CrossRef](#)] [[PubMed](#)]
42. Vetter, V.; Denizer, G.; Friedland, L.R.; Krishnan, J.; Shapiro, M. Understanding modern-day vaccines: What you need to know. *Ann. Med.* **2018**, *50*, 110–120. [[CrossRef](#)] [[PubMed](#)]

43. Nuwarda, R.F.; Alharbi, A.A.; Kayser, V. An Overview of Influenza Viruses and Vaccines. *Vaccines* **2021**, *9*, 1032. [[CrossRef](#)] [[PubMed](#)]
44. Sano, K.; Ainai, A.; Suzuki, T.; Hasegawa, H. Intranasal inactivated influenza vaccines for the prevention of seasonal influenza epidemics. *Expert. Rev. Vaccines* **2018**, *17*, 687–696. [[CrossRef](#)] [[PubMed](#)]
45. Benfield, T.L.; Helweg-Larsen, J. [SARS-CoV-2 vaccines]. *Ugeskr. Laeger* **2021**, *183*, V01210052. [[PubMed](#)]

Disclaimer/Publisher's Note: The statements, opinions and data contained in all publications are solely those of the individual author(s) and contributor(s) and not of MDPI and/or the editor(s). MDPI and/or the editor(s) disclaim responsibility for any injury to people or property resulting from any ideas, methods, instructions or products referred to in the content.